International Journal of Innovative
Computing, Information and Control
Volume **21**, Number **5**, October **2025**

ICIC International ©2025 ISSN 1349-4198
pp. **1467–1482**

OPTIMAL COST DESIGN FOR HOLLOW CIRCULAR FOOTINGS ASSUMING THAT THE GROUND CONTACT SURFACE IS PARTIALLY COMPRESSED

Inocencio Luévanos-Soto[1], Arnulfo Luévanos-Rojas[2,*]
and Rosa Margarita Luévanos-Soto[2]

[1]Facultad de Ingeniería, Ciencias y Arquitectura
Universidad Juárez del Estado de Durango, Unidad Gómez Palacio
Av. Universidad S/N, Fracc. Filadelfia, CP 35010, Gómez Palacio, Durango, México
inocencio.luevanos@ujed.mx

[2]Instituto de Investigaciones Multidisciplinaria
Facultad de Contaduría y Administración
Universidad Autónoma de Coahuila, Unidad Torreón
Blvd. Revolución 151 Ote. CP 27000, Torreón, Coahuila, México
r_luevanos@uadec.edu.mx
*Corresponding author: arnulfoluevanos@uadec.edu.mx

Received March 2025; revised June 2025

Abstract. *This paper presents a new model to obtain the minimum or optimal cost design for an annular strip footing or hollow circular footing to determine the steel areas and the effective depth, assuming that the soil is elastic, the soil pressure distribution is linear and the surface in contact with the soil works partially in compression. Some works assume uniform soil pressure and the external width of the foundation "w_1" is equal to the internal width of the foundation "w_2", and other authors show the optimal cost design for a solid circular footing taking into account that the area in contact with the soil works partially under compression. The formulations for the current model (Surface works entirely in compression) and the new model (Surface works partially in compression) are presented. Two numerical examples are shown to determine the optimal cost design for a hollow circular footing under an axial load and a resultant moment. A comparison between the current model and the new model is presented, and the results show that the new model is up to 0.0073 times smaller than the current model; therefore, greater saving can be achieved by using the new model.*
Keywords: Optimal cost design, Hollow circular footing, Linear soil pressure, Partially compressed contact surface

1. **Introduction.** A hollow circular footing or annular strip footing or ring footing is a shallow foundation used to support geometrically circular structures such as lighthouses, water or other liquid storage tank, wind turbines, grain storage silos, chimneys, and circular shaped auditoriums.

Figure 1 shows the distribution of soil pressure under a foundation according to the soil type and the foundation stiffness. Figure 1(a) presents a rigid foundation on sandy. Figure 1(b) shows a rigid foundation on clay. Figure 1(c) presents a flexible foundation on sandy. Figure 1(d) shows a flexible foundation on clay. Figure 1(e) presents a uniform distribution used in the current design [1].

The works that have been developed to determine the contact area with the ground for solid foundations subjected to biaxial bending are for isolated footings [2-11]; for

DOI: 10.24507/ijicic.21.05.1467

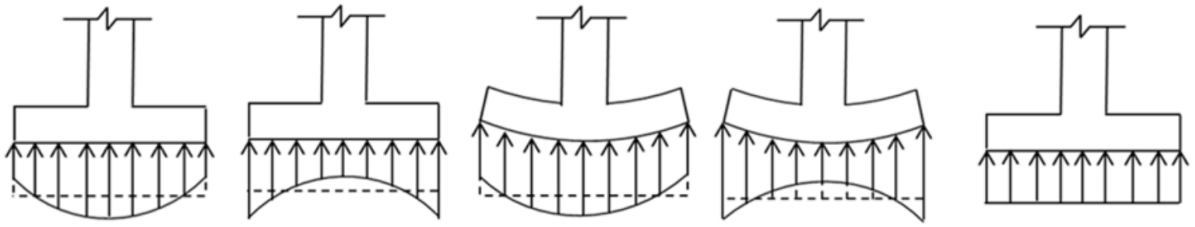

FIGURE 1. Distribution of the soil pressure under foundation

combined footings [12-16]. These papers assumed that the contact area works entirely in compression.

Various researchers have proposed complete designs for different types of solid foundations subjected to biaxial bending which are for isolated footings [17-21]; for combined footings [22-27]. All these works assumed that the contact area works entirely in compression.

Other works that have presented models to estimate the contact area for different types of solid foundations subjected to biaxial bending assuming that the contact area works partially to compression are for rectangular isolated footings [28-37]; for circular isolated footings [38-40]; for rectangular combined footings [41].

Some authors have estimated complete designs for different types of solid foundations subjected to biaxial bending assuming that soil contact surface works partially to compression which are for rectangular isolated footings [42] and for circular isolated footings [43].

The papers on hollow circular foundations or annular strip foundations or ring foundations are as follows. Singh-Rathor et al. [44] estimated a ring foundation based on the continuum approach and supported on reinforced concrete piles. Kim et al. [45] studied the bearing capacity of a ring foundation using the finite element method supported on moderately to highly weathered rocks. Sankaran and Subrahmanyam [46] developed an analytical solution for contact pressure distribution of a uniform load in ring foundations showing numerical examples and curves. Rathor and Sharma [47] investigated a comparison between ring slab foundations and solid slab foundations. Galvis and Smith-Pardo [48] obtained the coupled vertical load and biaxial moment capacity for circular and rectangular shallow foundations (ring and solid) by simplified closed-form equations with design aids. Ahmad et al. [49] analyzed the ring footings supported on elastic soil using finite difference technique. Rana and Jamani [50] investigated a comparison between ring slab foundations and solid slab foundations in water tank for different diameters. Kumar and Rai [51] analyzed a comparison between ring slab foundations without annular beam and with annular beam. Manideep et al. [52] estimated the bearing capacity of circular footings, ring footings and strip footings with limited soil depth.

According to the bibliography review carried out here, there are several works on solid foundations assuming that the area in contact with the ground works partially in compression, and other works on ring foundations working completely in compression. Therefore, there is no paper on optimal cost design for hollow circular footings assuming that the contact surface with soil works partially to compression.

This paper presents a model to determine the optimal cost design of an annular strip footing or hollow circular footing assuming that contact surface with the ground works partially in compression to obtain the steel areas and the effective depth, and this model is developed from data known as A_{min} (minimum area), R (radius), w_1 (external width

of the foundation) and w_2 (internal width of the foundation) proposed by Diaz-Gurrola et al. [53]. Some works show the optimal cost design of a solid circular footing, and others present annular strip footings or hollow circular footings assuming uniform soil pressure. In this work, two models are shown to determine the moments and shear forces: the current model (Area works entirely in compression) and the new model (Area works partially in compression). Two numerical examples are presented to estimate the optimal cost design for a hollow circular footing under an axial load P and a resultant moment M_R, and a comparison is also made between the current model and the new model to observe the differences.

The paper is organized as follows. Section 2 describes the formulation of the model to determine the optimal cost design of a hollow circular footing (current model and new model) assuming that contact surface with the ground works partially to compression. Section 2.1 shows the current model (Surface works entirely in compression). Section 2.2 presents the new model (Surface works partially in compression). Section 2.3 shows the optimal cost design for a hollow circular footing. Section 3 presents the numerical examples applied to the two models for a hollow circular footing. Section 4 shows the results. Section 5 presents the conclusions to complete the paper.

2. **Formulation of the Model.** Figure 2 shows a hollow circular footing subjected to a factored load and two factored moments.

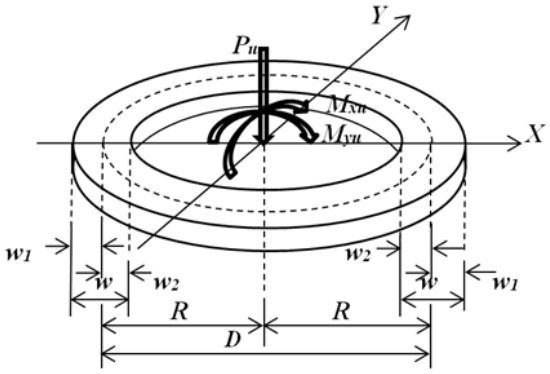

FIGURE 2. Hollow circular foundation for a factored load and two factored moments

General equation to determine the factored soil pressure "p_{su}" on the footing is

$$p_{su} = \frac{P_u}{A} + \frac{M_{xu}y}{I_x} + \frac{M_{yu}x}{I_y} \tag{1}$$

where A = contact area of the footing with ground, P_u = factored axial load, M_{xu} and M_{yu} = factored moments about each axis, x and y = coordinates of the base under study, I_x and I_y = moments of inertia about each axis. $P_u = 1.2P_D$ (dead load) + $1.6P_L$ (live load), $M_{xu} = 1.2M_{xD}$ (dead load moment) + $1.6M_{xL}$ (live load moment), $M_{yu} = 1.2M_{yD}$ (dead load moment) + $1.6M_{yL}$ (live load moment) [54].

Now, to simplify the work, a moment "M_{Ru}" (factored resultant moment) is determined from the factored moments "M_{xu}" and "M_{yu}".

Figure 3 shows "P_u", "M_{Ru}", "w" (total width of ring footing), "w_1" (external width of ring footing measured from center of wall), "w_2" (internal width of ring footing measured from center of wall), "R" (radius of the ring footing to the center of the wall) and "D" (diameter of the ring footing to the outer edge of the wall).

Now, "M_{Ru}" is determined as follows:

$$M_{Ru} = \sqrt{M_{xu}^2 + M_{yu}^2} \tag{2}$$

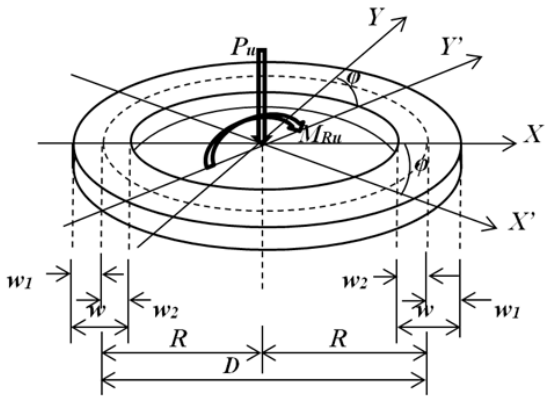

FIGURE 3. Hollow circular foundation for a factored load and the factored resultant moment

The inclination angle "φ" of the Y' axis with respect to the Y axis is determined as follows:

$$\cos\varphi = \frac{M_{xu}}{M_{Ru}} \rightarrow \varphi = \arccos\left(\frac{M_{xu}}{M_{Ru}}\right) \tag{3}$$

Now, substituting Equation (2) into Equation (1) is determined the factored soil pressure on the hollow circular foundation as follows:

$$p_{su} = \frac{P_u}{A} + \frac{M_{Ru}y}{I} \tag{4}$$

where y = coordinate of the foundation on the Y' axis.

Substituting $A = \pi(R+w_1)^2 - \pi(R-w_2)^2$ and $I = \pi(R+w_1)^4/4 - \pi(R-w_2)^4/4$ into Equation (4), the factored pressure "p_{su}" at any point on a hollow circular foundation is obtained:

$$p_{su} = \frac{P_u}{\pi[(R+w_1)^2 - (R-w_2)^2]} + \frac{4M_{Ru}y}{\pi[(R+w_1)^4 - (R-w_2)^4]} \tag{5}$$

The analysis width where the moments and shear forces are determined is detailed below (see Figure 4):

$$\cos\left(\frac{\alpha}{2}\right) = \frac{R+e}{R+w_1} \rightarrow \alpha = 2\arccos\left(\frac{R+e}{R+w_1}\right) \tag{6}$$

where α = angle of analysis, e = distance from R to where the analysis width is desired.

The analysis width where the moments and shear forces are generated is

$$s = (R+e)\alpha \tag{7}$$

2.1. **Case I. Surface works entirely in compression (Current model).** Figure 5 shows the critical sections where the factored critical moments and factored critical shear forces of a hollow circular footing appear.

The factored moment with respect to the "a" axis is obtained from the pressure generated by the soil and the area delimited by the ring formed from the radius "$R + b/2$" to "$R + w_1$".

The factored moment on the "a" axis "M_{au}" is

$$M_{au} = -2\int_{R+\frac{b}{2}}^{R+w_1}\int_{0}^{\frac{(R+w_1)\alpha}{2}} p_{su}\left(y - R - \frac{b}{2}\right)dxdy \tag{8}$$

where b = wall width, p_{su} is given by Equation (5).

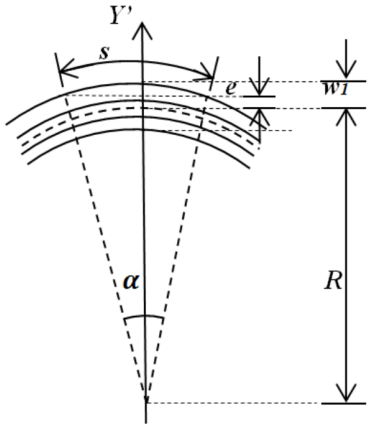

FIGURE 4. Analysis width for hollow circular foundation

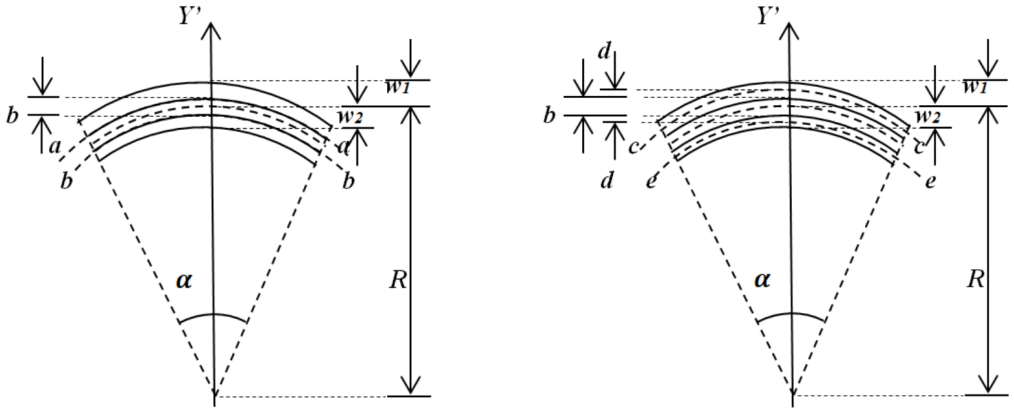

(a) Factored critical moments (b) Factored critical shear forces

FIGURE 5. Current model for a hollow circular foundation

The factored moment with respect to the "b" axis is obtained from $P_{\alpha u}$ multiplied by $b/2$ minus the pressure generated by the soil and the area delimited by the ring formed from the radius "$R - b/2$" to "$R + w_1$".

The factored moment on the "b" axis "M_{bu}" is

$$M_{bu} = \frac{P_{\alpha u} b}{2} - 2 \int_{R-\frac{b}{2}}^{R+w_1} \int_0^{\frac{(R+w_1)\alpha}{2}} p_{su} \left(y - R - \frac{b}{2} \right) dxdy \tag{9}$$

where $P_{\alpha u}$ is obtained by the following equation:

$$P_{\alpha u} = 2 \int_{R-w_2}^{R+w_1} \int_0^{\frac{(R+w_1)\alpha}{2}} p_{su} dxdy \tag{10}$$

where $P_{\alpha u}$ is the pressure generated by the soil on the area delimited by the ring formed from the radius "$R - w_2$" to "$R + w_1$".

The factored shear force on the "c" axis is obtained from the pressure generated by the soil and the area delimited by the ring formed from the radius "$R + b/2 + d$" to "$R + w_1$".

The factored shear force on the "c" axis "V_{cu}" is

$$V_{cu} = -2 \int_{R+\frac{b}{2}+d}^{R+w_1} \int_0^{\frac{(R+w_1)\alpha}{2}} p_{su} dxdy \tag{11}$$

The factored shear force on the "e" axis is obtained from $P_{\alpha u}$ minus the pressure generated by the soil and the area delimited by the ring formed from the radius "$R - b/2 - d$" to "$R + w_1$".

The factored shear force on the "e" axis "V_{eu}" is

$$V_{eu} = P_{\alpha u} - 2\int_{R-\frac{b}{2}-d}^{R+w_1}\int_{0}^{\frac{(R+w_1)\alpha}{2}} p_{su}\,dxdy \tag{12}$$

2.2. **Case II. Surface works partially in compression (New model).** Figure 6 shows the critical sections where the factored critical moments and factored critical shear forces of a hollow circular footing appear.

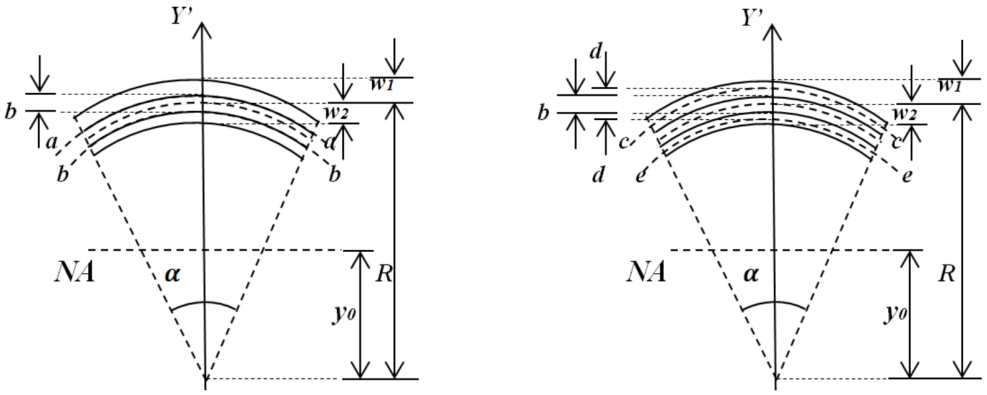

(a) Factored critical moments (b) Factored critical shear forces

FIGURE 6. New model for a hollow circular foundation

The factored pressure at anywhere of the footing "p_{zu}" using Equation (9) of Diaz-Gurrola et al. [53] is obtained:

$$p_{zu} = \frac{p_{maxu}(y - y_0)}{R + w_1 - y_0} \tag{13}$$

where p_{maxu} = factored maximum pressure, y = coordinate of the foundation on the Y' axis, y_0 = distance from X axis to neutral axis.

The values of p_{maxu} and y_0 are obtained from Equations (20) and (27) of Diaz-Gurrola et al. [53], substituting P_u, M_{Ru}, R, w_1 and w_2 in these two equations.

The factored moment with respect to the "a" axis is obtained from the pressure generated by the soil and the area delimited by the ring formed from the radius "$R + b/2$" to "$R + w_1$".

The factored moment on the "a" axis "M_{au}" is

$$M_{au} = -2\int_{R+\frac{b}{2}}^{R+w_1}\int_{0}^{\frac{\sqrt{(R+w_1)^2-y^2}}{2}} p_{zu}\left(y - R - \frac{b}{2}\right)dxdy \tag{14}$$

where p_{zu} is given by Equation (13).

The factored moment with respect to the "b" axis is obtained from $P_{\alpha u}$ multiplied by $b/2$ minus the pressure generated by the soil and the area delimited by the ring formed from the radius "$R - b/2$" to "$R + w_1$".

The factored moment on the "b" axis "M_{bu}" is

$$M_{bu} = \frac{P_{\alpha u}b}{2} - 2\int_{R-\frac{b}{2}}^{R+w_1}\int_{0}^{\frac{\sqrt{(R+w_1)^2-y^2}}{2}} p_{zu}\left(y - R - \frac{b}{2}\right)dxdy \tag{15}$$

where $P_{\alpha u}$ is obtained by the following equation:

$$P_{\alpha u} = 2\int_{R-w_2}^{R+w_1}\int_{0}^{\frac{\sqrt{(R+w_1)^2-y^2}}{2}} p_{zu}dxdy \tag{16}$$

where $P_{\alpha u}$ is the pressure generated by the soil on the area delimited by the ring formed from the radius "$R - w_2$" to "$R + w_1$".

The factored shear force on the "c" axis is obtained from the pressure generated by the soil and the area delimited by the ring formed from the radius "$R+b/2+d$" to "$R+w_1$".

The factored shear force on the "c" axis "V_{cu}" is

$$V_{cu} = -2\int_{R+\frac{b}{2}+d}^{R+w_1}\int_{0}^{\frac{\sqrt{(R+w_1)^2-y^2}}{2}} p_{zu}dxdy \tag{17}$$

The factored shear force on the "e" axis is obtained from $P_{\alpha u}$ minus the pressure generated by the soil and the area delimited by the ring formed from the radius "$R - b/2 - d$" to "$R + w_1$".

The factored shear force on the "e" axis "V_{eu}" is

$$V_{eu} = P_{\alpha u} - 2\int_{R-\frac{b}{2}-d}^{R+w_1}\int_{0}^{\frac{\sqrt{(R+w_1)^2-y^2}}{2}} p_{zu}dxdy \tag{18}$$

2.3. **Optimal cost design for a hollow circular footing.**

2.3.1. *Objective function.* The equation to determine the optimal cost "C_{op}" for the two cases is

$$C_{op} = V_c C_c + V_s \gamma_s C_s \tag{19}$$

where V_c = volume of concrete, C_s = cost of steel, V_s = volume of steel, γ_s = density of steel = 78 kN/m^3.

The reinforcing steel of a ring footing is constructed in one radial direction "A_{sR}" and in the other direction it is perimeter "A_{sT}".

The volume of reinforcing steel is

$$V_s = (2R + w_1 - w_2)\pi A_{sT} + \frac{2\pi(w_1+w_2)A_{sR}}{\alpha} \tag{20}$$

The volume of concrete is

$$V_c = \pi\left[(R+w_1)^2 - (R-w_2)^2\right](d+r) - \left[(2R + w_1 - w_2)\pi A_{sT} + \frac{2\pi(w_1+w_2)A_{sR}}{\alpha}\right] \tag{21}$$

Substituting V_s, V_c and the value of γ_s into Equation (19) gives

$$C_{op} = \left\{\pi\left[(R+w_1)^2 - (R-w_2)^2\right](d+r) - \left[(2R + w_1 - w_2)\pi A_{sT} + \frac{2\pi(w_1+w_2)A_{sR}}{\alpha}\right]\right\} C_c + \left[(2R + w_1 - w_2)\pi A_{sT} + \frac{2\pi(w_1+w_2)A_{sR}}{\alpha}\right]\gamma_s C_s \tag{22}$$

Now, substituting $\beta = \gamma_s C_s / C_c \rightarrow \gamma_s C_s = \beta C_c$ into Equation (22) gives

$$C_{op} = \pi\left[(R+w_1)^2 - (R-w_2)^2\right](d+r)C_c - \left[(2R + w_1 - w_2)\pi A_{sT} + \frac{2\pi(w_1+w_2)A_{sR}}{\alpha}\right](1-\beta)C_c \tag{23}$$

2.3.2. *Constraint functions.* Simplified equations for foundations design according to the American Concrete Institute standard code are shown below [54].

For moments:

$$|M_{au}|, |M_{bu}| \leq \emptyset_f f_y d A_s \left(1 - \frac{A_s f_y}{1.7 b_w d f'_c}\right) \tag{24}$$

where A_s (steel area for bending), b_w (analysis width for bending), f_y (specified yield strength of reinforcement of steel), f'_c (specified compressive strength of the concrete at 28 days), $\emptyset_f = 0.90$ (bending strength reduction factor). "A_s and b_w" for M_{au} correspond to "A_{sRa}" and "b_{wa}", and "A_s and b_w" for M_{bu} correspond to "A_{sRb}" and "b_{wb}". $b_{wa} = \alpha(R + b/2)$ and $b_{wb} = \alpha(R - b/2)$.

For shear forces:

$$|V_{cu}|, |V_{eu}| \leq 0.17 \emptyset_v \sqrt{f'_c} b_{ws} d \tag{25}$$

where b_{ws} (analysis width for shear force). "b_{ws}" for V_{cu} corresponds to "b_{wc}", and "b_{ws}" for V_{eu} corresponds to "b_{we}". $b_{wc} = \alpha(R + b/2 + d)$ and $b_{we} = \alpha(R - b/2 - d)$.

For steel percentages:

$$\rho_{Ra}, \rho_{Rb} \leq 0.75 \left[\frac{0.85 \beta_1 f'_c}{f_y} \left(\frac{600}{600 + f_y}\right)\right] \tag{26}$$

$$\rho_{Ra}, \rho_{Rb} \geq \begin{cases} \dfrac{0.25\sqrt{f'_c}}{f_y} \\ \dfrac{1.4}{f_y} \end{cases} \tag{27}$$

$$0.65 \leq \beta_1 = \left(1.05 - \frac{f'_c}{140}\right) \leq 0.85 \tag{28}$$

where ρ_{Ra} = percentage of steel for the width "b_{wa}", ρ_{Rb} = percentage of steel for the width "b_{wb}".

For steel areas:

$$A_{sRa} = \rho_{Ra} b_{wa} d \tag{29}$$

$$A_{sRb} = \rho_{Rb} b_{wb} d \tag{30}$$

$$A_{sR} \geq \begin{cases} A_{sRa} \\ A_{sRb} \end{cases} \tag{31}$$

$$A_{sT} = 0.0018(w_1 + w_2) d \tag{32}$$

Figure 7 shows the flowchart for determining the minimum cost of a hollow circular footing for the two cases using Maple software (Nonlinear optimization).

The general procedure to determine the optimal cost or minimum cost is used as follows:

The first step is to determine the minimum area using the procedure proposed by Diaz-Gurrola et al. [53].

The second step is to use the flowchart shown in Figure 7 to determine the optimal cost or minimum cost.

3. **Numerical Problems.** Two numerical examples are presented to determine the thickness, the radial steel area "A_{sR}" and the perimeter steel area "A_{sT}" of a hollow circular footing. Example 1 ($w_1 \neq w_2$) and Example 2 ($w_1 = w_2$) are developed for the same loads and moments, and each example presents five variants in p_{max} of 100, 150, 200, 250 and 300 kN/m^2. The examples are based on examples 1 and 2 of the data obtained from the work proposed by Diaz-Gurrola et al. [53]. The known parameters are $R = 20.00$ m, $P_D = 12000$ kN, $P_L = 8000$ kN, $M_{xD} = 0$ kN-m, $M_{xL} = 0$ kN-m, $M_{yD} = 200000$ kN-m,

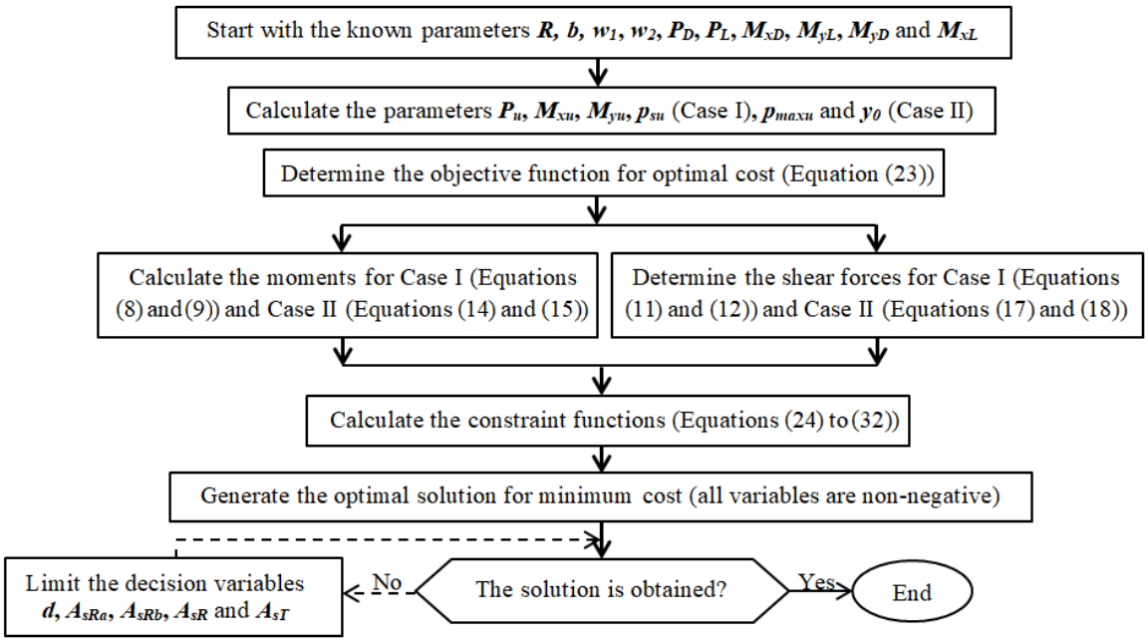

FIGURE 7. Flowchart for minimum cost of a hollow circular footing

$M_{yL} = 15000$ kN-m. The factored axial load and factored moments about each axis are determined: $P_u = 27200$ kN, $M_{xu} = 0$ kN-m, $M_{yu} = 480000$ kN-m, $M_{Ru} = 480000$ kN-m. The value of "p_{maxu}" is obtained from Equation (5) for Case I and the values of "p_{maxu}" and "y_0" are obtained from Equations (20) and (27) for Case II of Diaz-Gurrola et al. [53].

Table 1 shows the width and factored pressure of each footing and Table 2 presents the steel area and effective depth of each footing for $w_1 \neq w_2$ of example 1.

Table 3 shows the width and factored pressure of each footing and Table 4 presents the steel area and effective depth of each footing for $w_1 = w_2$ of example 2.

4. **Results.** Tables 1 and 3 are the data obtained in Tables 2 and 3 by Diaz-Gurrola et al. [53].

TABLE 1. Width and factored pressure of each footing (Example 1)

Type	Case	p_{max} (kN/m^2)	w_1 (m)	w_2 (m)	w (m)	p_{smax} (kN/m^2)	y_0 (m)	p_{maxu} (kN/m^2)	y_0 (m)
1	I	100	44.39	1.00	45.39	3.36	–	4.59	–
	II		4.37	1.00	5.37	100.00	1.25	138.69	1.86
2	I	150	44.39	1.00	45.39	3.36	–	4.59	–
	II		2.97	1.00	3.97	150.00	3.94	209.12	4.58
3	I	200	44.39	1.00	45.39	3.36	–	4.59	–
	II		2.18	1.00	3.18	200.00	5.48	279.65	6.13
4	I	250	44.39	1.00	45.39	3.36	–	4.59	–
	II		1.66	1.00	2.66	250.00	6.49	351.04	7.16
5	I	300	44.39	1.00	45.39	3.36	–	4.59	–
	II		1.30	1.00	2.30	300.00	7.21	420.71	7.87

where p_{max} = unfactored allowable soil pressure, p_{smax} = unfactored pressure generated by the soil on the footing, p_{maxu} = factored pressure generated by the soil on the footing.

TABLE 2. Steel area and effective depth of each footing (Example 1)

Type	Case	Solution	d (cm)	A_{sR} (cm^2)	A_{sT} (cm^2)	ρ_{Ra}	ρ_{Rb}	A_{sRa} (cm^2)	A_{sRb} (cm^2)	C_{op}
1	I	First	89.44	9390.80	730.74	0.02073	0.02125	9390.80	9390.80	11741.21
		Second	92.00	8983.95	715.66	0.01928	0.01976	8983.95	8983.95	12040.14
	II	First	23.41	1101.83	22.63	0.01969	0.02019	1101.83	1101.83	233.61
		Second	27.00	900.05	26.10	0.01395	0.00649	900.05	408.39	259.26
2	I	First	89.44	9390.80	730.74	0.02073	0.02125	9390.80	9390.80	11741.21
		Second	92.00	8983.95	715.66	0.01928	0.01976	8983.95	8983.95	12040.14
	II	First	33.56	402.16	23.98	0.00528	0.00617	352.70	402.16	218.90
		Second	37.00	360.92	26.44	0.00431	0.00502	317.49	360.92	236.82
3	I	First	89.44	9390.80	730.74	0.02073	0.02125	9390.80	9390.80	11741.21
		Second	92.00	8983.95	715.66	0.01928	0.01976	8983.95	8983.95	12040.14
	II	First	19.89	403.76	11.39	0.01045	0.01223	353.95	403.76	115.82
		Second	22.00	356.36	12.59	0.00844	0.00976	315.99	356.36	124.39
4	I	First	89.44	9390.80	730.74	0.02073	0.02125	9390.80	9390.80	11741.21
		Second	92.00	8983.95	715.66	0.01928	0.01976	8983.95	8983.95	12040.14
	II	First	17.54	237.64	8.40	0.00878	0.00945	226.38	237.64	87.39
		Second	22.00	183.04	10.53	0.00541	0.00581	175.02	183.04	102.45
5	I	First	89.44	9390.80	730.74	0.02073	0.02125	9390.80	9390.80	11741.21
		Second	92.00	8983.95	715.66	0.01928	0.01976	8983.95	8983.95	12040.14
	II	First	19.14	114.67	7.93	0.00469	0.00481	114.67	114.67	79.35
		Second	22.00	98.71	9.11	0.00351	0.00341	98.71	93.41	87.65

TABLE 3. Width and factored pressure of each footing (Example 2)

Type	Case	p_{max} (kN/m^2)	w_1 (m)	w_2 (m)	w (m)	p_{smax} (kN/m^2)	y_0 (m)	p_{maxu} (kN/m^2)	y_0 (m)
1	I	100	–	–	–	–	–	–	–
	II		3.75	3.75	7.50	100.00	5.80	140.22	6.39
2	I	150	–	–	–	–	–	–	–
	II		2.49	2.49	4.98	150.00	6.93	210.74	7.56
3	I	200	–	–	–	–	–	–	–
	II		1.84	1.84	3.68	200.00	7.39	281.16	8.03
4	I	250	–	–	–	–	–	–	–
	II		1.45	1.45	2.90	250.00	7.60	351.80	8.26
5	I	300	–	–	–	–	–	–	–
	II		1.19	1.19	2.38	300.00	7.72	423.58	8.39

Table 1 presents the following: In Case I, all values of w_1, w_2, w and p_{smax} are equal for any "p_{max}", because the soil pressure is governed by minimum pressure which is zero. In Case II, when "p_{max}" increases, "y_0" and "p_{maxu}" increase, and "p_{max}" = "p_{smax}".

Table 2 (taking account of the second solution which is the final solution) shows the following: In Case I, all values of d, A_{sR}, A_{sT}, ρ_{Ra}, ρ_{Rb}, A_{sRa}, A_{sRb} and C_{op} are equal for all types of "p_{max}". In Case II, when "p_{max}" increases, A_{sR}, A_{sRa}, A_{sRb} and C_{op} decrease, ρ_{Ra} and ρ_{Rb} decrease until type 2 and then increase in type 3 and subsequently decrease, A_{sT} increases until type 2 and then decreases, d increases until type 2 and then they are equal.

TABLE 4. Steel area and effective depth of each footing (Example 2)

Type	Case	Solution	d (cm)	A_{sR} (cm^2)	A_{sT} (cm^2)	ρ_{Ra}	ρ_{Rb}	A_{sRa} (cm^2)	A_{sRb} (cm^2)	C_{op}
1	I	First	–	–	–	–	–	–	–	–
		Second	–	–	–	–	–	–	–	–
	II	First	28.24	538.50	38.12	0.00856	0.00876	538.50	536.98	343.94
		Second	32.00	446.15	43.20	0.00654	0.00333	466.15	231.64	379.19
2	I	First	–	–	–	–	–	–	–	–
		Second	–	–	–	–	–	–	–	–
	II	First	28.63	253.04	25.66	0.00485	0.00496	253.04	252.35	230.23
		Second	32.00	224.27	28.68	0.00384	0.00339	224.27	192.92	251.30
3	I	First	–	–	–	–	–	–	–	–
		Second	–	–	–	–	–	–	–	–
	II	First	27.82	153.64	18.43	0.00355	0.00364	153.64	153.64	166.23
		Second	32.00	165.86	21.20	0.00333	0.00342	165.86	165.86	185.63
4	I	First	–	–	–	–	–	–	–	–
		Second	–	–	–	–	–	–	–	–
	II	First	26.51	154.77	13.84	0.00334	0.00440	120.69	154.77	126.26
		Second	27.00	151.74	14.09	0.00333	0.00423	122.50	151.74	128.04
5	I	First	–	–	–	–	–	–	–	–
		Second	–	–	–	–	–	–	–	–
	II	First	24.95	162.56	10.69	0.00536	0.00552	161.75	162.56	98.97
		Second	27.00	149.02	11.57	0.00333	0.00467	108.97	149.02	105.10

Table 3 presents the following: In Case I, there is no value because w_2 is insufficient to obtain a minimum area. In Case II, when "p_{max}" increases, "y_0" and "p_{maxu}" increase, and "p_{max}"="p_{smax}".

Table 4 (taking account of the second solution which is the final solution) shows the following: In Case I, there is no value because w_2 is insufficient to obtain a minimum area. In Case II, when "p_{max}" increases, A_{sR}, A_{sRa}, A_{sRb}, A_{sT} and C_{op} decrease, ρ_{Ra} decreases until type 3 and then they are equal, ρ_{Rb} increases, d is equal until type 3 and then in types 4 and 5 is equal.

Figure 8 presents in detail the general diagram of a hollow circular foundation. Figure 9 shows the comparison between Case I (current model) and Case II (new model) under the concept of minimum cost.

As seen in Figure 9, there are major differences between the current model and the new model according to the minimum cost. The smallest difference is presented at p_{max} = 100 kN/m^2 of 12040.14/259.26 = 46.44 times the current model with respect to the new model. The largest difference is presented at p_{max} = 300 kN/m^2 of 12040.14/87.65 = 137.37 times the current model with respect to the new model.

5. **Conclusions.** This paper presents a new model to obtain the minimum or optimal cost design for an annular strip footing or hollow circular footing to determine the steel areas and the effective depth, assuming that the soil is elastic, the soil pressure distribution is linear and the surface in contact with the soil works partially in compression.

This model is developed from data known as A_{min}, R, w_1 and w_2 proposed by Diaz-Gurrola et al. [53].

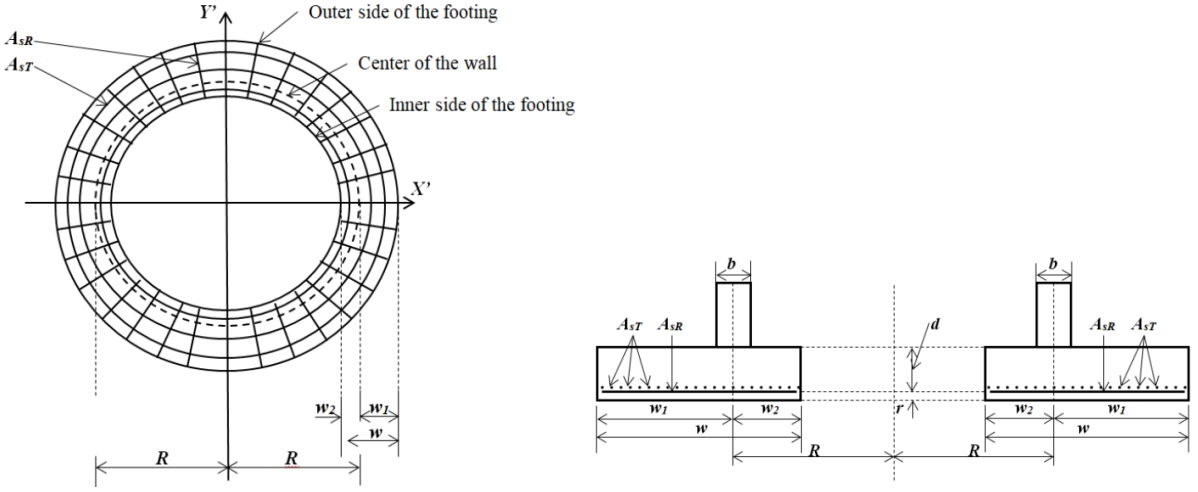

(a) Plan view (b) Elevation view

FIGURE 8. Diagram of a hollow circular foundation

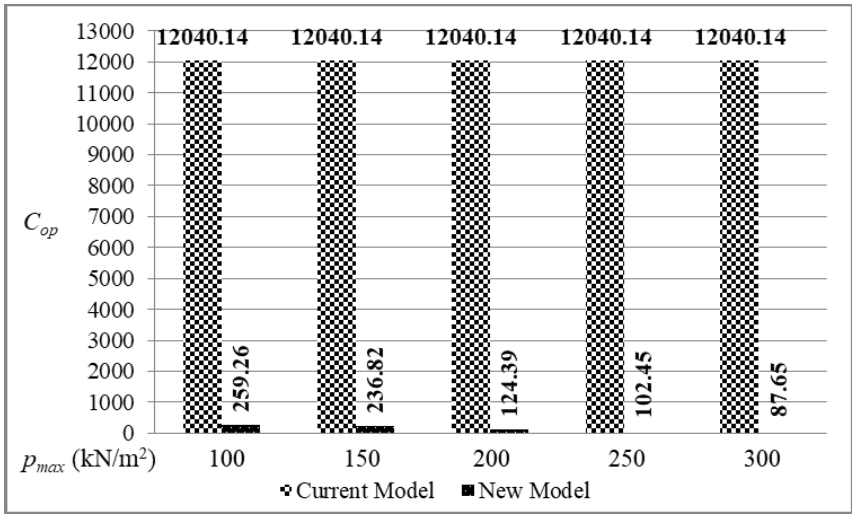

FIGURE 9. Comparison between the current model and the new model

The contributions of this work are as follows.

1) Some works assume uniform soil pressure, and the external width of the foundation "w_1" is equal to the internal width of the foundation "w_2".

2) The optimal cost for the new model (case II) is 0.0215 times that of the current model (case I) at $p_{max} = 100$ kN/m^2, 0.0197 times that of the current model at $p_{max} = 150$ kN/m^2, 0.0103 times that of the current model at $p_{max} = 200$ kN/m^2, 0.0085 times that of the current model at $p_{max} = 250$ kN/m^2, 0.0073 times that of the current model at $p_{max} = 300$ kN/m^2 (see Figure 9).

3) Greater savings are achieved when the allowable soil load capacity "p_{max}" is increased (see Figure 9).

4) Tables 3 and 4 do not show results for Case I, because it is not possible to obtain an area that satisfies the conditions, since w_2 was greater than R, which is not possible.

The suggestions for the next research are

1) Optimal area for a hollow rectangular footing assuming that the contact surface with soil works partially under compression;

2) Optimal cost for a hollow rectangular footing assuming that the contact surface with soil works partially under compression.

REFERENCES

[1] J. E. Bowles, *Foundation Analysis and Design*, McGraw-Hill, New York, USA, 2001.

[2] J. Khazaie and S. A. Amirshahkarami, Numerical analysis of interaction between earth and large foundations regarding size effect, *Journal of Applied Sciences*, vol.9, no.6, pp.1036-1045, 2009.

[3] M. Jahanandish, M. Veiskarami and A. Ghahramani, Effect of foundation size and roughness on the bearing capacity factor, N_γ, by stress level-based ZEL method, *Arabian Journal for Science and Engineering*, vol.37, no.7, pp.1817-1831, 2012.

[4] G. A. Vyacheslavovich and B. L. Adolfovich, Influence of the form and size of the isolated foundations on the stress-strain state of the soil base, *Journal of Applied Engineering Science*, vol.14, no.1, pp.28-35, 2016.

[5] S. López-Chavarría, A. Luévanos-Rojas and M. Medina-Elizondo, A mathematical model for dimensioning of square isolated footings using optimization techniques: General case, *International Journal of Innovative Computing, Information and Control*, vol.13, no.1, pp.67-74, 2017.

[6] S. López-Chavarría, A. Luévanos-Rojas and M. Medina-Elizondo, Optimal dimensioning for the corner combined footings, *Advances in Computational Design*, vol.2, no.2, pp.169-183, 2017.

[7] A. Luévanos-Rojas, A mathematical model for dimensioning of footings square, *International Review of Civil Engineering*, vol.3, no.4, pp.346-350, 2012.

[8] A. Luévanos-Rojas, A mathematical model for the dimensioning of circular footings, *Far East Journal of Mathematical Sciences*, vol.71, no.2, pp.357-367, 2012.

[9] A. Luévanos-Rojas, A mathematical model for dimensioning of footings rectangular, *ICIC Express Letters, Part B: Applications*, vol.4, no.2, pp.269-274, 2013.

[10] W. L. Filho, R. C. H. Carvalho, A. L. Christoforo and F. A. R. Lahr, Dimensioning of isolated footing submitted to the under biaxial bending considering the low concrete consumption, *International Journal of Materials Engineering*, vol.7, no.1, pp.1-11, 2017.

[11] A. Luévanos-Rojas, A comparative study for dimensioning of footings with respect to the contact surface on soil, *International Journal of Innovative Computing, Information and Control*, vol.10, no.4, pp.1313-1326, 2014.

[12] A. Luévanos-Rojas, A new mathematical model for dimensioning of the boundary trapezoidal combined footings, *International Journal of Innovative Computing, Information and Control*, vol.11, no.4, pp.1269-1279, 2015.

[13] A. Luévanos-Rojas, A mathematical model for the dimensioning of combined footings of rectangular shape, *Revista Técnica de la Facultad de Ingeniería Universidad del Zulia*, vol.39, no.1, pp.3-9, 2016.

[14] A. Luévanos-Rojas, S. López-Chavarría and M. Medina-Elizondo, A new model for T-shaped combined footings Part I: Optimal dimensioning, *Geomechanics and Engineering*, vol.14, no.1, pp.51-60, 2018.

[15] G. Aguilera-Mancilla, A. Luévanos-Rojas, S. López-Chavarría and M. Medina-Elizondo, Modeling for the strap combined footings Part I: Optimal dimensioning, *Steel and Composite Structures*, vol.30, no.2, pp.97-108, 2019.

[16] M. A. Moreno-Hernandez, A. Luévanos-Rojas, S. López-Chavarría and M. Medina-Elizondo, Mathematical modeling for corner strap combined footings resting on the ground: Part 1, *Computación y Sistemas*, vol.26, no.3, pp.1259-1272, 2022.

[17] A. Luévanos-Rojas, J. G. Faudoa-Herrera, R. A. Andrade-Vallejo and M. A. Cano-Alvarez, Design of isolated footings of rectangular form using a new model, *International Journal of Innovative Computing, Information and Control*, vol.9, no.10, pp.4001-4022, 2013.

[18] S. López-Chavarría, A. Luévanos-Rojas and M. Medina-Elizondo, A new mathematical model for design of square isolated footings for general case, *International Journal of Innovative Computing, Information and Control*, vol.13, no.4, pp.1149-1168, 2017.

[19] A. Luévanos-Rojas, Design of isolated footings of circular form using a new model, *Structural Engineering and Mechanics*, vol.52, no.4, pp.767-786, 2014.

[20] A. Luévanos-Rojas, Minimum cost design for rectangular isolated footings taking into account that the column is located in any part of the footing, *Buildings*, vol.13, no.9, pp.1-16, 2023.

[21] A. Luévanos-Rojas, V. M. Moreno-Landeros, G. Santiago-Hurtado, F. J. Olguin-Coca, L. D. López-León and E. R. Diaz-Gurrola, Mathematical modeling for the optimal cost design of circular isolated footings with eccentric column, *Mathematics*, vol.12, no.5, pp.1-19, 2024.

[22] A. Luévanos-Rojas, Design of boundary combined footings of rectangular shape using a new model, *DYNA Colombia*, vol.81, no.188, pp.199-208, 2014.
[23] A. Luévanos-Rojas, S. López-Chavarría and M. Medina-Elizondo, A new model for T-shaped combined footings Part II: Mathematical model for design, *Geomechanics and Engineering*, vol.14, no.1, pp.61-69, 2018.
[24] J. A. Yáñez-Palafox, A. Luévanos-Rojas, S. López-Chavarría and M. Medina-Elizondo, Modeling for the strap combined footings Part II: Mathematical model for design, *Steel and Composite Structures*, vol.30, no.2, pp.109-217, 2019.
[25] M. L. Garcia-Graciano, A. Luévanos-Rojas, S. López-Chavarría and M. Medina-Elizondo, Mathematical modeling for corner strap combined footings resting on the ground: Part 2, *Computación y Sistemas*, vol.26, no.4, pp.1429-1443, 2022.
[26] A. Luévanos-Rojas, Optimization for trapezoidal combined footings: Optimal design, *Advances in Concrete Construction*, vol.16, no.1, pp.21-34, 2023.
[27] A. Luévanos-Rojas, G. Santiago-Hurtado, V. M. Moreno-Landeros, F. J. Olguin-Coca, L. D. López-León and E. R. Diaz-Gurrola, Mathematical modeling of the optimal cost for the design of strap combined footings, *Mathematics*, vol.12, no.2, pp.1-20, 2024.
[28] R. Irles-Más and F. Irles-Más, Alternativa analítica a la determinación de tensiones bajo zapatas rectangulares con flexión biaxial y despegue parcial (Explicit stresses under rectangular detached footings with biaxial bending), *Informes de la Construcción*, vol.44, no.419, pp.77-90, 1992.
[29] H. M. Algin, Stresses from linearly distributed pressures over rectangular areas, *International Journal Numerical Analytical Methods in Geomechanics*, vol.24, no.8, pp.681-692, 2000.
[30] H. M. Algin, Practical formula for dimensioning a rectangular footing, *Engineering Structures*, vol.29, no.6, pp.1128-1134, 2007.
[31] G. Özmen, Determination of base stresses in rectangular footings under biaxial bending, *Teknik Dergi Digest*, vol.22, no.4, pp.1519-1535, 2011.
[32] J. Bellos and N. P. Bakas, High computational efficiency through generic analytical formulation for linear soil pressure distribution of rigid spread rectangular footings, *Proc. of the 7th European Congress on Computational Methods in Applied Sciences and Engineering*, Crete Island, Greece, 2016.
[33] J. Bellos and N. P. Bakas, Complete analytical solution for linear soil pressure distribution under rigid rectangular spread footings, *International Journal of Geomechanics*, vol.17, no.7, DOI: 10.1061/(ASCE)GM.1943-5622.0000874, 2017.
[34] I. Aydogdu, New iterative method to calculate base stress of footings under biaxial bending, *International Journal of Engineering & Applied Sciences (IJEAS)*, vol.8, no.4, pp.40-48, 2016.
[35] K. Girgin, Simplified formulations for the determination of rotational spring constants in rigid spread footings resting on tensionless soil, *Journal of Civil Engineering and Management*, vol.23, no.4, pp.464-474, 2017.
[36] V. B. Vela-Moreno, A. Luévanos-Rojas, S. López-Chavarría, M. Medina-Elizondo, R. Sandoval-Rivas and C. Martínez-Aguilar, Optimal area for rectangular isolated footings considering that contact surface works partially to compression, *Structural Engineering and Mechanics*, vol.84, no.4, pp.561-573, 2022.
[37] V. M. Moreno-Landeros, A. Luévanos-Rojas, G. Santiago-Hurtado, L. D. López-León and E. R. Diaz-Gurrola, Optimal area for a rectangular isolated footing with an eccentric column and partial ground compression, *Applied Sciences*, vol.14, no.15, pp.1-16, 2024.
[38] S. Soto-Garcia, A. Luévanos-Rojas, J. D. Barquero-Cabrero, S. López-Chavarría, M. Medina-Elizondo, O. M. Farias-Montemayor and C. Martínez-Aguilar, A new model for the contact surface with soil of circular isolated footings considering that the contact surface works partially under compression, *International Journal of Innovative Computing, Information and Control*, vol.18, no.4, pp.1103-1116, 2022.
[39] I. Luévanos-Soto, A. Luévanos-Rojas, V. M. Moreno-Landeros and G. Santiago-Hurtado, Minimum area for circular isolated footings with eccentric column taking into account that the surface in contact with the ground works partially in compression, *Coupled Systems Mechanics*, vol.13, no.3, pp.201-217, 2024.
[40] A. Luévanos-Rojas, B. L. Estrada-Mendoza and M. Juárez-Ramirez, Comparative study for minimum areas in contact with the ground of rectangular and circular isolated footings working partially under compression, *Boletín Ciencias de la Tierra*, vol.55, no.1, pp.85-98, 2024.

[41] P. Montes-Paramo, A. Luévanos-Rojas, S. López-Chavarría, M. Medina-Elizondo and R. Sandoval-Rivas, Optimal area for rectangular combined footings assuming that contact surface with the soil works partially to compression, *Ingeniería Investigación y Tecnología*, vol.24, no.2, pp.1-15, 2023.

[42] A. Luévanos-Rojas, New model for complete design of rectangular isolated footings taking into account that the contact surface works partially in compression, *Revista ALCONPAT*, vol.10, no.3, pp.192-219, 2023.

[43] D. S. Kim-Sanchez, A. Luévanos-Rojas, J. D. Barquero-Cabrero, S. López-Chavarría, M. Medina-Elizondo and I. Luévanos-Soto, A new model for the complete design of circular isolated footings considering that the contact surface works partially under compression, *International Journal of Innovative Computing, Information and Control*, vol.18, no.6, pp.1769-1784, 2022.

[44] A. P. Singh-Rathor, J. K. Sharma and M. Madhira, An analytical study of annular raft on granular piles, *Studia Geotechnica et Mechanica*, vol.46, no.1, pp.21-44, 2024.

[45] B. S. Kim, O. Kwon, Y. H. Choi and J. K. Lee, Bearing capacity of annular foundations on rock mass with heterogeneous disturbance by finite element limit analysis, *Buildings*, vol.12, no.5, pp.1-11, 2022.

[46] K. S. Sankaran and M. S. Subrahmanyam, Analytical solution for annular ring-uniform loading contact pressure distribution to predict machine foundation response, *Soils and Foundations*, vol.13, no.3, pp.17-27, 1973.

[47] A. P. S. Rathor and J. K. Sharma, Engineering significance of annular raft foundations over solid raft foundations, *International Journal for Research in Applied Science & Engineering Technology*, vol.11, no.9, pp.930-934, 2023.

[48] F. A. Galvis and J. P. Smith-Pardo, Axial load biaxial moment interaction (PMM) diagrams for shallow foundations: Design aids, experimental verification, and examples, *Engineering Structures*, vol.213:110582, 2020.

[49] S. K. Ahmad, V. Srinivasan and P. Ghosh, Analysis of annular footings and anchors lying on elastic soil medium using finite difference technique, *The 5th International Congress on Computational Mechanics and Simulation*, 2014.

[50] Y. Rana and A. Jamani, Comparative study of annular raft foundation & solid circular raft foundation for different diameter of water tank, *International Research Journal of Engineering and Technology*, vol.5, no.4, pp.3428-3436, 2018.

[51] R. Kumar and A. Rai, F.E.M analysis of annular mat foundation with & without annular beam, *International Research Journal of Engineering and Technology*, vol.10, no.10, pp.103-107, 2023.

[52] R. Manideep, A. V. R. Karthik and J. T. Chavda, Bearing capacity of strip, circular and ring footings on limited depth of soil, *Journal of GeoEngineering*, vol.18, no.4, pp.203-214, 2023.

[53] E. R. Diaz-Gurrola, A. Luévanos-Rojas, G. J. Montiel-Sánchez and C. Martínez-Aguilar, Optimal surface in plan for hollow circular footings assuming that the contact surface with soil works partially under compression, *International Journal of Innovative Computing, Information and Control*, vol.21, no.2, pp.407-422, 2025.

[54] ACI 318-19 (American Concrete Institute), *Building Code Requirements for Structural Concrete and Commentary*, Committee 318, New York, USA, 2019.

Author Biography

Inocencio Luévanos-Soto obtained his Bachelor's degree in Architect in 2009, his Master's degree in Science with Specialization in Planning and Construction of Works in 2012, and his Doctor degree in Engineering with Specialization in Planning Systems and Construction in 2024, all from Facultad de Ingeniería, Ciencias y Arquitectura, Gómez Palacio Campus of the Universidad Juárez del Estado de Durango, México. He is professor and researcher of the Facultad de Ingeniería, Ciencias y Arquitectura, Gómez Palacio Campus of the Universidad Juárez del Estado de Durango, México from since 2010 to date. His research interests are mathematical models applied to engineering and architect.

Arnulfo Luévanos-Rojas obtained his Bachelor's degree in Civil Engineering in 1981 from Facultad de Ingeniería, Ciencias y Arquitectura, Gómez Palacio Campus of the Universidad Juárez del Estado de Durango, México, his Master's degree in Science with Specialization in Structures in 1983 from Instituto Politécnico Nacional, Distrito Federal, México, his Master's degree in Science with Specialization in Planning and Construction of Works in 2000 from Facultad de Ingeniería, Ciencias y Arquitectura, Gómez Palacio Campus of the Universidad Juárez del Estado de Durango, México, his Master's degree in Administration in 2004 from Facultad de Contaduría y Administración, Torreón Campus of the Universidad Autónoma de Coahuila, México, and his Doctor degree in Engineering with Specialization in Planning Systems and Construction in 2009 from Facultad de Ingeniería, Ciencias y Arquitectura, Gómez Palacio Campus of the Universidad Juárez del Estado de Durango, México. He was professor and researcher of the Facultad de Ingeniería, Ciencias y Arquitectura, Gómez Palacio Campus of the Universidad Juárez del Estado de Durango, México from 2006 to 2015, and of the Facultad de Contaduría y Administración, Torreón Campus of the Universidad Autónoma de Coahuila, México since 2015 to date. He has published more than 146 papers in journals indexed in the Web of Science. His research interests are mathematical models applied to engineering and administration. He is member of the National System of Researchers of Mexico (Level I from 2016-2022 and Level II from 2023-2027). He is an Honorary State Researcher for the State of Coahuila, Mexico. He has received several distinctions: Distinguished Professor by ULSA (Universidad La Salle Laguna) 2002, 2007, 2010; Researcher of the year 2023 by UAC (Universidad Autónoma de Coahuila); Best scientific article of the year 2023 by UAC (Universidad Autónoma de Coahuila); He has been included in the "2023 World's Top 2% Scientists List" by Stanford University, Mathematical Engineering Excellence Award by Math Scientist Awards (2025).

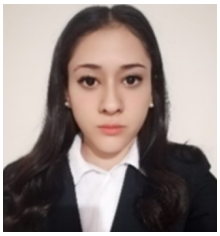

Rosa Margarita Luévanos-Soto received the Master's degree in Administration and Senior Management (2020) and the degree of Doctor in Administration and Senior Management (2024) from the Facultad de Contaduría y Administración of the Universidad Autónoma de Coahuila, México. She is professor and researcher of the Facultad de Contaduría y Administración, Torreón Campus of the Universidad Autónoma de Coahuila, México. Her research interests are mathematical models applied to administration.